Biomedicine & Pharmacotherapy 162 (2023) 114627

Contents lists available at ScienceDirect

Biomedicine & Pharmacotherapy

journal homepage: www.elsevier.com/locate/biopha

Abrogation of stemness in osteosarcoma by the mithramycin analog EC-8042 is mediated by its ability to inhibit NOTCH-1 signaling

Óscar Estupiñán [a,b], Verónica Rey [a,b,c], Juan Tornín [a,b], Dzohara Murillo [a,b], Borja Gallego [a,b], Carmen Huergo [a,b], Verónica Blanco-Lorenzo [a,b,d], M. Victoria González [a,b,c,e], Aida Rodríguez [a,b], Francisco Moris [f], Jessica González [c,g,h], Verónica Ayllón [i,j], Verónica Ramos-Mejía [i], Anna Bigas [c,g,h], René Rodríguez [a,b,c,*,1]

[a] Instituto de Investigación Sanitaria del Principado de Asturias (ISPA), Hospital Universitario Central de Asturias, Avenida de Roma, s/n 33011, Oviedo, Spain
[b] Instituto Universitario de Oncología del Principado de Asturias, 33011 Oviedo, Spain
[c] CIBER en oncología (CIBERONC), 28029 Madrid, Spain
[d] Servicio de Anatomía Patológica, Hospital Universitario Central de Asturias, 33011 Oviedo, Spain
[e] Departamento de Cirugía, Universidad de Oviedo, 33006 Oviedo, Spain
[f] EntreChem SL, 33011 Oviedo, Spain
[g] Program in Cancer Research, Institut Hospital del Mar d'Investigacions Mèdiques, Barcelona, Spain
[h] Josep Carreras Leukemia Research Institute, Barcelona, Spain
[i] GENYO - Centre for Genomics and Oncological Research - Pfizer/University of Granada/Junta de Andalucía, Granada, Spain
[j] Departamento de Biología Celular, Facultad de Ciencias, Universidad de Granada, 18071 Granada, Spain

ARTICLE INFO

Keywords:
NOTCH1
HES1
EC-8042
Mithramycin
Sarcoma
Osteosarcoma
Cancer stem cells

ABSTRACT

Osteosarcomas are frequently associated to a poor prognosis and a modest response to current treatments. EC-8042 is a well-tolerated mithramycin analog that has demonstrated an efficient ability to eliminate tumor cells, including cancer stem cell subpopulations (CSC), in sarcomas. In transcriptomic and protein expression analyses, we identified NOTCH1 signaling as one of the main pro-stemness pathways repressed by EC-8042 in osteosarcomas. Overexpression of NOTCH-1 resulted in a reduced anti-tumor effect of EC-8042 in CSC-enriched 3D tumorspheres cultures. On the other hand, the depletion of the NOTCH-1 downstream target HES-1 was able to enhance the action of EC-8042 on CSCs. Moreover, HES1 depleted cells failed to recover after treatment withdrawal and showed reduced tumor growth potential in vivo. In contrast, mice xenografted with NOTCH1-overexpressing cells responded worse than parental cells to EC-8042. Finally, we found that active NOTCH1 levels in sarcoma patients was associated to advanced disease and lower survival. Overall, these data highlight the relevant role that NOTCH1 signaling plays in mediating stemness in osteosarcoma. Moreover, we demonstrate that EC-8042 is powerful inhibitor of NOTCH signaling and that the anti-CSC activity of this mithramycin analog highly rely on its ability to repress this pathway.

Abbreviations: ABCC1, ATP Binding Cassette Subfamily C Member 1; AKT1, AKT Serine/Threonine Kinase 1; CCL2, C-C Motif Chemokine Ligand 2; CCND1, Cyclin D1; CDH4, Cadherin 4; CFU, Colony formation unit assays; C-MYC, MYC Proto-Oncogene BHLH Transcription Factor; CSC, Cancer stem cell; CXCL, C-X-C Motif Chemokine Ligand; DEG, differential expressing genes; Emax, Percentage of maximum effect; HES1, Hairy Enhancer of Split Family BHLH Transcription Factor 1; HEY, Hes Related Family BHLH Transcription Factors with YRPW Motif; IC_{50}, Concentration of half-maximal inhibition of viability; MAML, Mastermind Like Transcriptional Coactivator 1; MMP, Matrix Metallopeptidase; MTM, Mithramycin A; NICD, Notch intracellular domain; NOTCH1, Notch Receptor 1; PTK2, Protein Tyrosine Kinase 2; RBPJ, Recombination Signal Binding Protein for Immunoglobulin Kappa J Region; RPTOR, Regulatory Associated Protein Of MTOR Complex 1; RTV, Relative tumor volumes; SCG2, Secretogranin II; SOX, Sex-determining region Y-box protein; SP1, Specificity Protein 1; SRC, SRC Proto-Oncogene Non-Receptor Tyrosine Kinase; TERT, Telomerase Reverse Transcriptase; TGI, Tumor growth inhibition; THBS1, Thrombospondin 1; TM, Transmembrane; VEGFA, Vascular Endothelial Growth Factor A; WNT, Wingless-Type MMTV Integration Site Family.

* Correspondence to: Sarcomas and Experimental Therapeutics Lab., Instituto de Investigación Sanitaria del Principado de Asturias (ISPA), Av. de Roma s/n, 33011 Oviedo, Spain.
E-mail address: rene.rodriguez@ispasturias.es (R. Rodríguez).
[1] ORCID: 0000–0002-0768-7306

https://doi.org/10.1016/j.biopha.2023.114627
Received 13 January 2023; Received in revised form 15 March 2023; Accepted 29 March 2023
Available online 3 April 2023

1. Introduction

Osteosarcomas constitute the most common type of primary bone cancer [1,2]. Treatment of these neoplasms is currently based on the surgical removal of the primary tumor with wide-margin resection, with or without combinatory (neo)-adjuvant chemotherapy or radiation therapy [1,3]. Although localized tumors generally respond well to conventional treatments, a high proportion of cases eventually relapse and / or develop metastases, leading to overall survival rates that remain below 50% [1,3]. The frequent appearance of drug resistant clones, may be in part explained by the emergence of subsets of tumor cells presenting a stem cell-like phenotype. These Cancer Stem Cells (CSCs) has been identified and characterized in many tumors including osteosarcomas and has been widely associated with drug resistance, tumor relapses and metastasis development [4–6].

Different signaling pathways are known to mediate stemness both in normal stem cells and CSCs. Among them, the NOTCH pathway plays relevant roles in cell fate determination, differentiation and survival in development and tissue homeostasis [7]. This highly evolutionally conserved pathway is initiated by the binding of different Jagged or Delta-like ligands to a family of 4 transmembrane receptors (NOTCH1–4 in humans). This receptor-ligand interaction induces sequential cleavages of the Notch receptor which produce the release of the Notch intracellular domain (NICD) in the signal-receiving cell. Subsequently, NICD translocates to the nucleus, where it promotes the expression of target genes such as those coding for Hairy Enhancer of Split (HES) proteins, HES related proteins (HEY), CCND1 or C-MYC [7]. In osteosarcomas, altered expression and activation of NOTCH signaling has been reported to play a key role in tumor development [8], tumor growth [9], angiogenesis, metastasis [10,11], and the acquisition of drug resistance by CSCs subpopulations [12,13].

Mithramycin A (MTM), also known as Plicamycin, is a natural antitumoral antibiotic that binds preferentially to GC-rich sequences in DNA. By this mechanism, this drug blocks the binding of key oncogenic transcription factors, such as those of the SP family, to their promoters, thereby inhibiting the expression of their target genes [14,15]. MTM has shown a remarkable activity against various malignant neoplasms. In addition, several studies have evidenced the powerful ability of MTM to target CSCs in many types of cancers [16–22]. Nevertheless, this drug has been partially relegated out of clinical use because of its high toxicity [17]. To take advantage of these remarkable anti-tumor properties of MTM while minimizing its detrimental effects, second-generation MTM analogs with improved safety profiles have been developed [23]. A leading MTM analog generated by genetic engineering of the MTM biosynthesis pathways is EC-8042 (demycarosyl-3D-β-D-digitoxosyl-mithramycin SK) [24]. This compound has proven to be 10-fold less toxic than MTM [25] while showing a strong antitumor activity against Ewing Sarcoma [26], melanoma [27], ovarian cancer [28] and breast cancer [29]. In addition, it has been reported that EC-8042 is able to efficiently target CSCs in sarcomas [30,31], head and neck tumors [32], and prostate cancer [33].

Here we show that EC-8042 is an efficient multi-target repressor of NOTCH-1 signalling in sarcomas. Given the prominent roles that NOTCH signaling plays in the development and progression of osteosarcomas [34], here we focused to study the effect of EC-8042 in this type of sarcomas. We generated gain and/or loss of function models of osteosarcoma to demonstrate that EC-8042 ability to repress NOTCH signaling is a relevant anti-stemness mechanism of action of this MTM analog. Finally, we found that NOTCH1 expression was associated to a poorer outcome of sarcoma patients.

2. Materials and methods

2.1. Cell culture, lentiviral constructions and drugs

Transformed bone marrow-derived mesenchymal stem/stromal cell lines with expression of the myxoid liposarcoma-associated fusion gene FUS-CHOP were previously generated and characterized [35,36]. Osteosarcomas cell lines Saos-2, MG63, U2OS and 143B were obtained from the American Type Culture Collection (ATCC, Manassas, Virginia, USA). The identity of all cell lines has been authenticated by Short Tandem Repeats analysis within the last 3 months. All the cell lines were tested for Mycoplasma monthly using the Biotools Mycoplasma Gel Detection kit (B&M LABS, Spain) and cultured as previously described [37]. Sarcoma cell lines were stably modified to modulate the expression of NOTCH1 and HES1 by transduction with lentiviral particles obtained using a 3rd generation lentiviral packaging system and the following lentiviral vectors: 1) A lentiviral vector encoding the cDNA for the intracellular domain of NOTCH1 (N1ICD) (EF.v-CMV.GFP; Addgene, ref: 2,17623) lentiviral vectors encoding human HES1-specific shRNAs (SMARTvector Lentiviral shRNA, Refs: V3SH11240–225656557 (D9) and V3SH11240–226832480 (D10); Horizon Discovery, Cambridge, UK); and 3) an empty vector (pWPI; Addgene, ref:12254) used as control. Cells expressing these lentiviral vectors, which were positive for the fluorescence marker GFP, were selected by flow cytometry using BD FACS Aria II Cell Sorter (BD Bioscience, Erembodegem, Belgium). EC-8042 and MTM were synthesized using proprietary processes by EntreChem S.L. (Oviedo, Spain) [24] and used as previously described [31].

2.2. Tumorsphere culture

Tumorsphere formation protocol and the analysis of the effects of drugs on tumorsphere formation ability were previously described [38].

2.3. Cell viability assays

The viability of cell lines after the exposition to different drug concentrations for 48 h was determined using the cell proliferation reagent WST-1 (Roche, Mannheim, Germany) or by performing colony formation unit assays (CFU) as described before [17]. The concentration of half-maximal inhibition of viability (IC_{50}) and the maximum effect (E_{max}, percentage of growth inhibition reached with higher concentration assayed) was determined by non-linear regression using GraphPad Prism version 8.0 (Graphpad Software Inc, La Jolla, CA).

2.4. Analysis of cell proliferation

Real time cell proliferation was measured using a RTCA iCELLigence™ analyzer (Agilent Technologies, Santa Clara, CA) as previously described using 1×10^4 cells/well [39]. In some cases, 0.1 μM EC-8042 was added at the indicated times for 48 h. After this treatment, cell cultures were washed and let to grow in fresh medium for up to one week while being monitored by the RTCA iCELLigence™ system. Data collection and analysis was performed in the RTCA Data Analysis Software 1.0 and cell proliferation was presented as normalized cell index values.

2.5. Western blotting

Whole cell protein extraction and Western blot analysis were performed as previously described [40]. Primary antibodies used in these analyses were: anti-NOTCH1[EP1238Y] [(52627), 1:1000 dilution] from Abcam (Cambridge, UK); anti HES1 (E-5) [(sc-166410), 1:100] from Santa Cruz Biotechnology (Dallas, TX); anti-MAML1 (D3K7B) [(12166), 1:1000] from Cell Signaling (Beverly, MA); and anti-β-Actin [(A5441), 1:10,000] from Sigma Aldrich (San Louis, MI).

2.6. Transcriptome analysis

RNA sequencing analyses of triplicate samples obtained from cell cultures treated with EC-8042 and MTM was performed and analyzed as

previously described [17]. These RNA seq datasets are available in the GEO-NCBI repository (Reference: GSE161616; https:// www. ncbi. nlm. nih. gov/ geo/ query/ acc. cgi? acc= GSE16 1616).

2.7. RT-qPCR

RNA extraction and RT reactions were performed as previously described [30]. Gene expression was analyzed by real-time qPCR using 20 ng of cDNA, SYBR Green Master Mix protocol (Applied Biosystems, CA, USA) and 300 nM of primers in a StepOnePlus Real-Time PCR System (Applied Biosystems, CA, USA) at 95 °C for 10 min, followed by 40 cycles of 95 °C for 15 s, 60 °C for 30 s, and 72 °C for 30 s. Reactions were run in triplicates using the following specific primers: HES1 (Sigma) 5´-GCCTATTATGGAGAAAAGACG-3´(Fw) and 5´- GCCTATTATGGAGAAAAGACG-3´(Rv); MAML2 (Sigma) 5´- AATTGATGGGAAAGAAGCAG-3´(Fw) and 5´- CAATTTTCTCCGCGTCAG-3´(Rv); NOTCH1 (Thermo Fisher) 5´-CTACCTGTCAGACGTGGCCT-3´(Fw)and 5´- CGCAGAGGGTTGTATTGGTT-3´(Rv); RPTOR (Sigma) 5´-CGGAGTTTCCTTTAACAGTG-3´(Fw) and 5´- CTGTTGAGTACTTTCATGGC-3´(Rv); TGFB1 (Sigma) 5´- AACCCACAACGAAATCTATG-3´(Fw) and 5´- CTTTTAACTTGAGCCTCAGC-3´(Rv); VEGFA (Sigma) 5´-AATGTGAATGCAGACCAAAG-3´(Fw) and 5´- GACTTATACCGGGATTTCTTG-3´(Rv). And the ribosomal coding gene RPL19 5´-AGCGAGCTCTTTCCTTTCG-3´(Fw) and 5´-GAGCCTCTTCTGAAGCCTGA-3´(Rv) was used as endogenous control. The relative mRNA expression was calculated using the $2-\Delta\Delta CT$ method, and the data were expressed as the fold-change normalized to RPL19 mRNA levels and relative to control (vehicle-treated) cells.

2.8. In vivo tumor growth

Female Athymic nude mice of 6 weeks old (Envigo, Barcelona, Spain) were inoculated subcutaneously (s.c.) with 10^5 parental 143B, 143B-NICD, 143B-shD9 or 143B-shD10 cells. Once tumors reached approximately 100 mm^3, mice inoculated with the different cell lines were randomly assigned (n = 5 per group) to receive intra-venous (i.v.) treatments of saline solution (control) or EC-8042 at a dose of 18 mg/kg twice a week (6 doses). Mice were sacrificed by cervical dislocation at the end of this protocol. Mean tumor volume differences between groups were determined using a caliper and relative tumor volumes (RTV) and the percentage tumor growth inhibition (%TGI) were calculated as described [37]. Additionally, other cohorts of mice (n = 3 per group) carrying xenografts generated with 143B-parental, 143B-NICD and 143B-shD10 cells received four doses of treatments before tumors were extracted and processed for protein extraction.

2.9. Histological analysis

Paraffin-embedded tissues from 82 patients with sarcoma who underwent resection of their tumors at the Hospital Universitario Central de Asturias (HUCA) were used to construct a tissue microarray as previously described [41]. Immunostaining of NOTCH1 was performed using an anti-NOTCH1 antibody (#3608) from Cell Signaling (Danvers, MA) at 1:300 dilution. Stained samples were scored blinded to clinical data by a pathologist (VBL), using a semiquantitative scoring system based on both the percentage of stained cells (0: 0%; 1: <10%; 2: 10–50%; and 3: >50%) and the staining intensity (0: no expression; 1: low intensity; and 2: high intensity). Each sample received a scoring value resulting from the multiplication of both scores, and the median value in the resulting distribution was used to discriminate low and high expressing samples.

2.10. Statistical analyses

All data are represented as mean (± SD or SEM as indicated) of at least three independent experiments unless otherwise stated. Student's t or one-way ANOVA tests were performed to determine the statistical significance between groups. χ^2 test (with Yates' correction, when appropriate) was used in immunohistochemical analysis. Survival curves were calculated using the Kaplan-Meier product limit estimate and differences between survival times were analyzed by the log-rank method. Hazard Ratio (HR) was calculated by univariate Cox regression analysis. $p < 0.05$ values were considered statistically significant.

3. Results

3.1. EC-8042 acts as a multi-target repressor of NOTCH signaling in sarcoma cells

We first analyzed the anti-proliferative effect of EC-8042 in a panel of osteosarcoma cell lines. We found that all cell lines were sensitive to the effect of EC-8042, with 143B cells being the most sensitive (IC_{50} = 93 nM) (Fig. 1 A). This result is in line with our previous findings demonstrating an efficient anti-tumor activity of EC-8042 also in liposarcoma and undifferentiated pleomorphic sarcoma models, which displayed viability reduction IC_{50} values between 100 and 300 nM [30,31]. To reveal molecular mechanisms involved in the anti-tumor effect of EC-8042, we performed RNAseq analyses in the osteosarcoma cell line 143B and the myxoid liposarcoma model T-5H-FC#1 treated for 24 h with their respective IC_{50}'s. The analysis of differentially expressed genes (DEG) showed that EC-8042 induced a profound modulation of gene expression in both 143B (1368 DEGs) and T-5H-FC#1 (4757 DEGS) cells (Fig. 1B-C, Table S1 and Table S2). As expected, we found a high degree of overlapping between genes commonly regulated by EC-8042 in T-5H-FC#1 and 143B cells (65.69% of downregulated and 54.77% of overexpressed DEGS in 143B cells were also modulated in T-5H-FC#1 cells). Among relevant factors commonly downregulated by EC-8042 in both cell lines we found SP1 target genes such as VEGFA, PDGFA, ABCC1, RPTOR or TERT. Other commonly affected targets include cytokines as CXCL3 or CCL2, tyrosine kinases as SRC, PTK2 or AKT1, or other relevant signaling factors as NOTCH1, WNT5, WNT5B, TGFB1 or CDH4 (Fig. 1B-C, Table S1 and Table S2). The downregulation of selected genes by EC-8042 in both cell lines were confirmed by RT-qPCR (Fig. S1).

In concordance with its activity as transcription factor repressor, KEGG pathway analysis of DEGs show a predominant inhibitory effect of EC-8042 in sarcoma cells (Fig. 1D-E). Thus, most of the pathways significantly altered in T-5H-FC#1 (33 out of 34) (Fig. 1D and Table S3) and 143B cells (30 out of 31) (Fig. 1E and Table S4) were predicted to be repressed after the treatment. Most of these altered pathways, including key oncogenic pathways such as those controlled by NOTCH1, VEGF, WNT, Focal adhesion targets, or ECM receptor interaction factors, were commonly modulated in both cell lines (70% of overlap). Among these pathways, NOTCH signaling was consistently repressed by EC-8042 at different steps of the route in both T-5H-FC# 1 and 143B cells. This included the repression of receptors such as NOTCH1 and/or 2, different components of the transcriptional complex such as MAML factors, CREBBP or RBPJ and most of the well-known downstream targets of the pathway, like HES1, VEGFA, CXCL1, WNT5A or JUN (Fig. 2 A).

Western blotting analyses confirmed the ability of EC-8042 to repress the expression of several NOTCH signaling components in a panel of four osteosarcoma cell lines (Fig. 2B, Fig. S2A and Fig. S3A). We analyzed the expression of the two cleaved forms that originate during the process of activation of NOTCH1 upon ligand binding, a ≈120 kDa transmembrane (TM) form resulting from a first cleavage by ADAM proteases in the extracellular region and the ≈ 80–90 kDa NICD that is released in the cytosol after a second cleavage by γ-secretases. We detected a higher abundance of the TM form in all lines. EC-8042 induced a downregulation of both forms in all cell lines with the only exception of NICD in Saos2 and U2OS in which we did not observed a clear trend in the assayed conditions. We also, analyzed the expression of the transcriptional complex component MAML1 and the downstream target HES1.

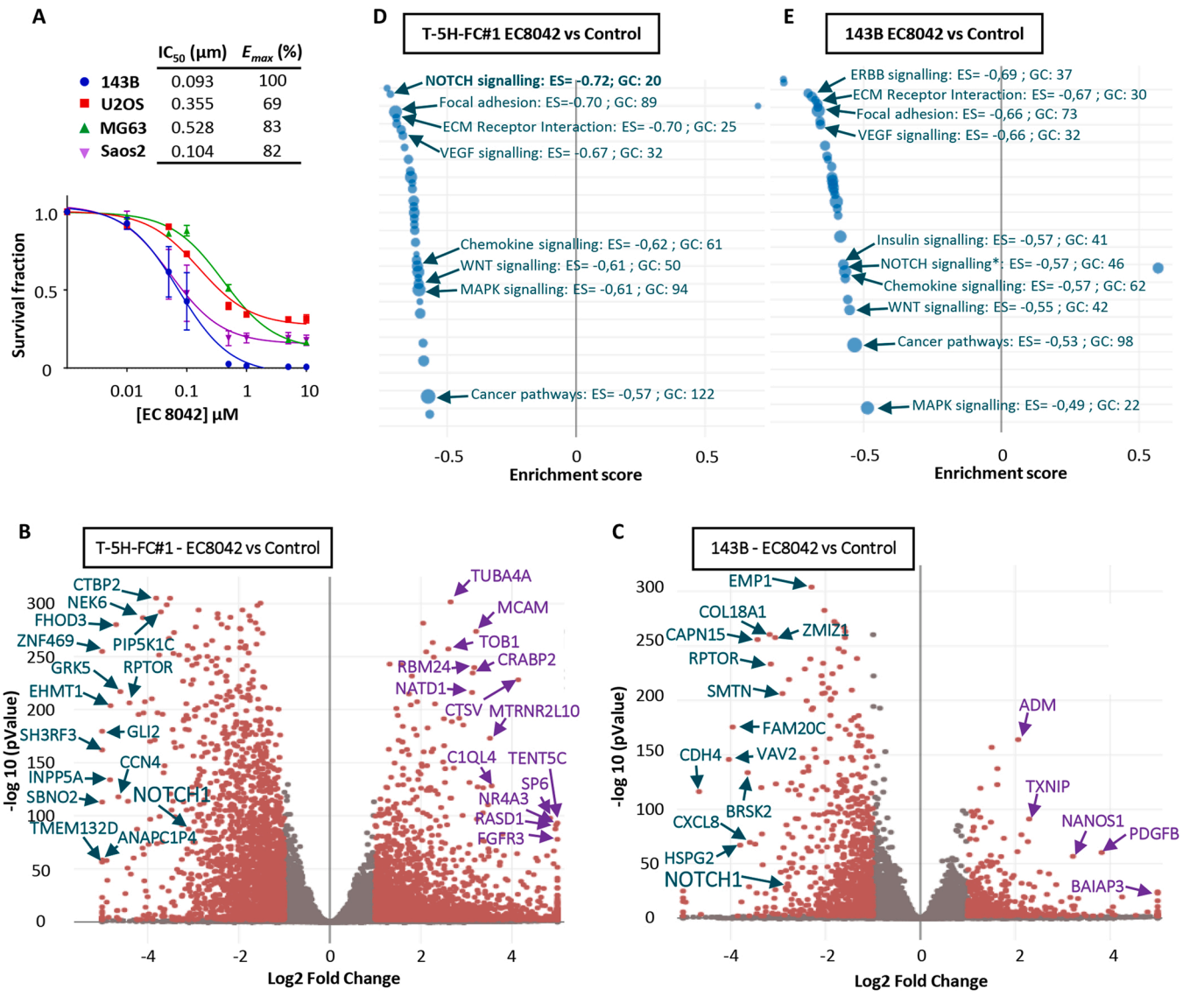

Fig. 1. Transcriptomic analysis of sarcoma cells treated EC-8042. (A) Cell viability (WST1 assay) measured after the treatment of a panel of osteosarcoma cell lines with increasing concentrations of EC-8042 for 48 h. The IC_{50} and maximum effect (E_{max}) values are shown. (B-E) RNAseq analysis of T-5H-FC#1 and 143B cells treated in triplicate with either DMSO (carrier control), or their respective IC_{50} for EC-8042 (300 nM for T-5H-FC#1 and 100 nM for 143B) for 24 h. (B-C) Volcano plots showing those genes significantly upregulated and downregulated (fold change (FC) ≤ -2 (log2 FC ≤ -1) or ≥ 2 (log2 FC ≥ 1) and padj < 0.01; red dots) when comparing EC-8042-treated vs control T-5H-FC#1 cells (B) and 143B cells (C). Selected relevant genes displaying highly significant p values and/or higher fold change modulation are indicated. (D-E) KEGG pathway analysis showing signaling routes significantly altered (enrichment score (ES) ≤ -0.5 or ≥ 0.5 and padj < 0.01; blue circles) when comparing EC-8042-treated vs control T-5H-FC#1 cells (D) and 143B cells (E). Circle diameter for each pathway reflect the number of genes involved in the pathway (gene count, GC) showing altered activation. Information for relevant cancer-related pathways is displayed.

Similar to NOTCH1, these proteins also follow a dose-dependent downregulation pattern (Fig. 2B). Similar results were also observed in an experiment where samples of all cell lines, treated or not with 1 μM EC-8042, were analyzed in the same blot (Fig. 2 C, Fig. S2B and Fig. S3B). In this experiment, we found that these factors were expressed at different levels in all cell lines and confirmed the ability of EC-8042 to inhibit the expression of NOTCH1 and HES1.

3.2. Modulation of NOTCH1 or Hes1 expression influences the recovery of osteosarcoma cells after the treatment with EC-8042

To study whether the ability of EC-8042 to inhibit NOTCH1 signaling plays any role in the anti-proliferative activity of this drug, we used a lentiviral vector in which NICD expression is controlled by a constitutive promoter that cannot be targeted by EC-8042 to generate a strain of 143B cells overexpressing active NOTCH1 (143B-N1ICD) (Fig. 3 A, Fig. S2C and Fig. S4A). Parallel, we silenced HES1 expression in 143B cells using two different shRNAs (143B-shD9 and 143B-shD10) (Fig. 3B, Fig. S2D and Fig. S4B). When treated with EC-8042 for 48 h in cell viability assays, we did not find significant changes in the sensitivity to this drug between NICD-overexpressing or HES1-depleted osteosarcoma cells and their respective control lines (Fig. 3 C). Similarly, we found that EC-8042 displayed a similar anti-clonogenic effect in all models in colony-forming assays (Fig. 3D-E). In these experiments, we did not observe significant differences in the clonogenic ability of control and NOTCH1-expression modulated cells in untreated conditions (Fig. S5A).

To further explore whether NOTCH1 signaling modulation produced any impact in the response of osteosarcoma cells to EC-8042, we analyzed the ability of parental, N1ICD-overexpressing and HES1-depleted 143B cells to recover after the treatment with EC-8042. For this purpose, we used the iCellingence™ system to follow the real time proliferation of the different cultures. First, we found that in untreated

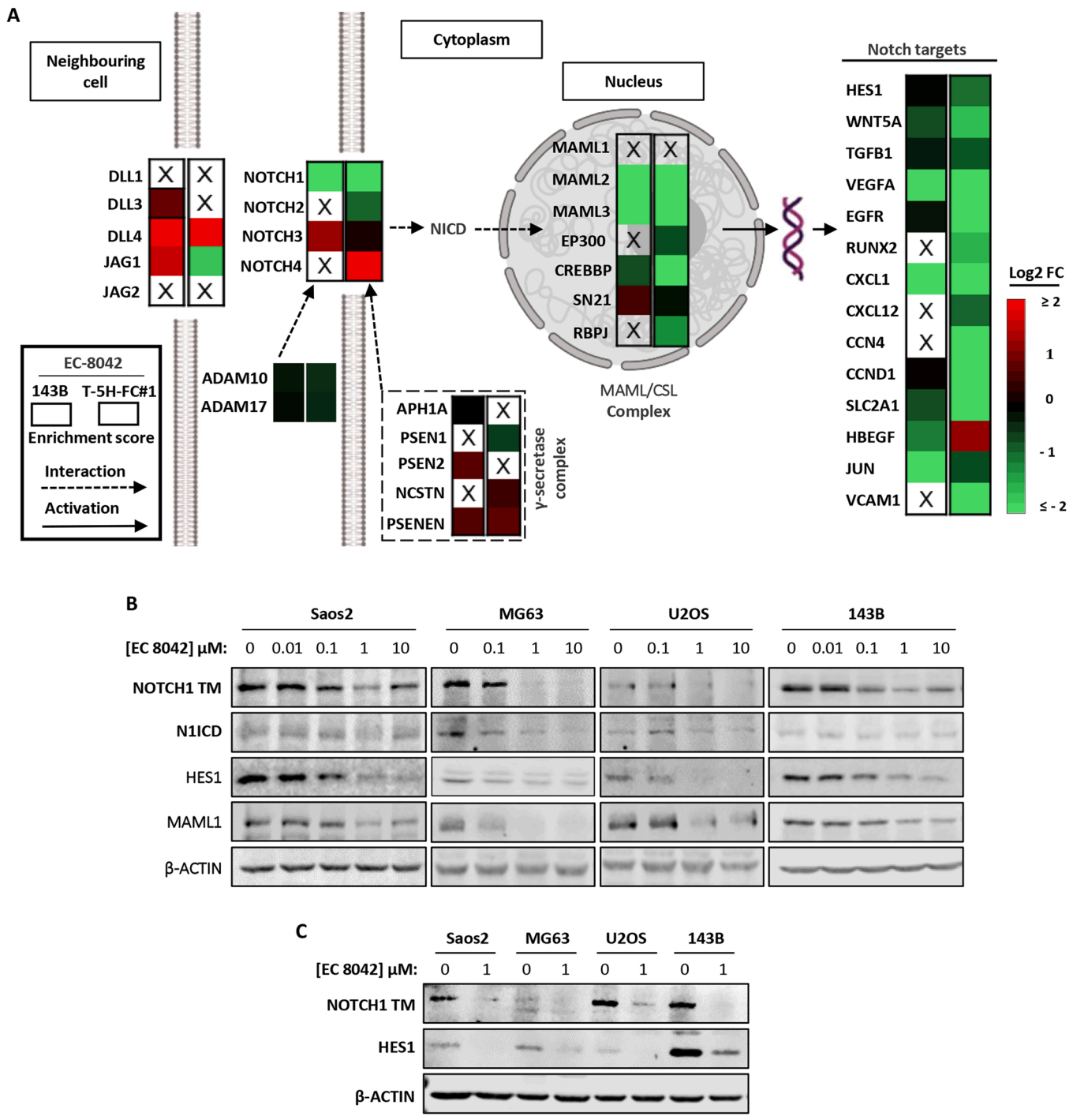

Fig. 2. Inhibition of NOTCH1 signaling by EC-8042 in sarcomas. (A) NOTCH1 signaling pathway scheme showing upregulation or downregulation levels of relevant components of the pathway in T-5H-FC#1 and 143B cells treated with EC-8042 in comparison with control cells. Green and red colors indicate significant downregulation and upregulation, respectively. Targets with non-significant p-values are labeled with an X. (B) Western blotting analyses of relevant components of the NOTCH1 pathway in a panel of osteosarcoma cell lines treatment with increasing concentrations of EC-8042 for 24 h. (C) Similar analysis of the expression of NOTCH1-related factors in samples of the different osteosarcoma cell lines treated or not with 1 μm EC-8042 for 24 h and loaded in the same blot. The expression of β-actin was used as loading control.

conditions, 143B-shD9 cells proliferate slightly faster than control or NICD-overexpressing cells (Fig S5B). When exposed to 0.25 μM EC-8042 for 48 h, we found parental 143B proliferated slightly faster during the treatment and showed a weaker response to EC-8042 than the rest of models (Fig. 3 F). When we analyzed how the different models recovered cell growth once the drug was removed, we noticed that although the control 143B cells recover earlier than the rest of models, most likely due to its poorer response, 143-NICD cells showed a more robust recovery and was able to reach higher level of confluence than that reached by control cells. More strikingly, both cell lines with silenced HES1 expression did not show any recover of cell growth after the removal of EC-8042 (Fig. 3 F).

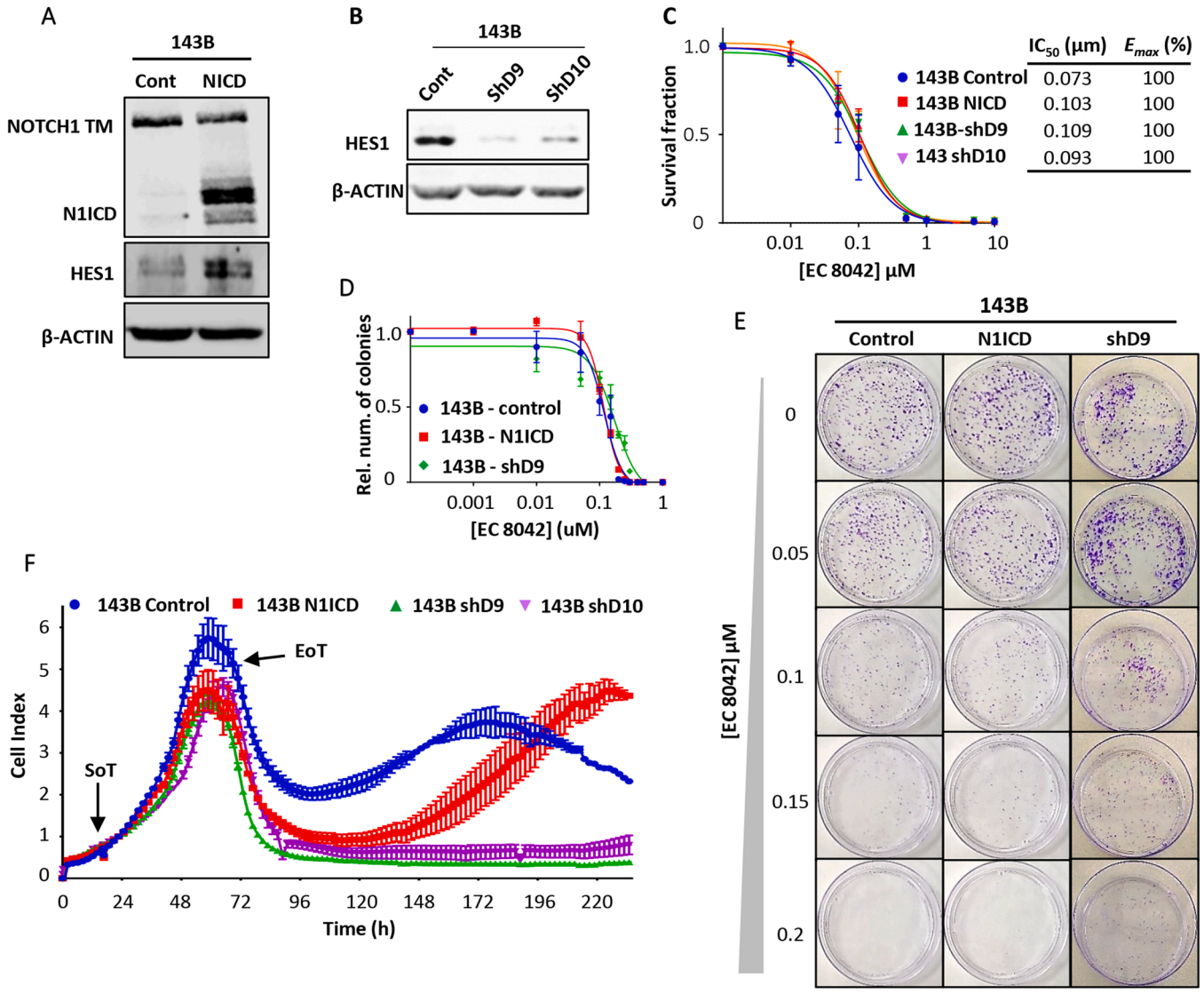

Fig. 3. Effect of the modulation of NOTCH1 signaling in the antiproliferative effect of EC-8042 in osteosarcoma cell lines. (A) Protein expression levels of NOTCH1 (TM and NICD forms) in control (Cont) and NICD-overexpressing (NICD) 143B cells. (B) Protein expression levels of control and HES1-silenced (shD9 and shD10) 143B cells. β-actin was used as loading control for western blotting analysis. (C) Cell viability assay of NOTCH1-signaling modified 143B cells treated with increasing concentrations of EC-8042 for 48 h. IC_{50} and E_{max} values are shown. (D-E) Colony formation unit (CFU) assays for control and NOTCH1-signaling modified 143B cells treated with increasing concentrations of EC-8042 for 24 h before letting them to form CFUs for 10 days. Summary graphic (D) and representative images of CFU assays for each condition (E) are shown. (F) Real time proliferation (cell index) of parental and NOTCH1-signaling modified 143B cells treated with 0.25 µM EC-8042 for 48 h and left to recover in fresh medium for one week. SoT and EoT indicated the start and the end of treatment respectively. Error bars represent the standard deviation of at three replicates. The panel shows the results of one of two independent experiments performed that showed similar results.

3.3. NOTCH-1 signaling inhibition plays a key role in the anti-CSC activity of EC-8042

The differential ability to recover after the treatment with EC-8042 could be related with the distinct ability of the drug to target CSCs in sarcoma cells with enhanced or impaired NOTCH1 signaling. To determine the role of NOTCH1 signaling in the response of sarcoma CSCs to EC-8042, we grew cultures of CSC-enriched 3D tumorspheres [31,42] from parental 143B, 143B-NICD, 143B-shD9 y 143B-shD10 cells and treated them with increasing concentrations of EC-8042. We found that tumorspheres formed by parental 143B cells were highly sensitive to the anti-stemness activity of EC-8042 (IC_{50} = 34 nM). Importantly, we also found that 143B-NICD-formed tumorspheres (IC_{50} = 248 nM) were approximately 7.5 times less sensitive than parental cells (Fig. 4A-B). In addition, although in untreated conditions HES1-silenced cells formed significantly less tumorspheres than parental 143B or 143B-NICD cells (Fig. 4 C), 143B-shD9 and 143B-shD10 tumorspheres seemed to respond similar than parental cells to the treatment with EC-8042 (Fig. 4A-B).

To further explore how the modulation of NOTCH1 signaling affects the anti-stemness potential of EC-8042, we treated adherent cultures from all 143B models with increasing concentrations of EC-8042 for 48 h and then grew them under CSC culture conditions to assay the formation of tumorspheres. Again, we found that EC-8042 was able to efficiently eliminate CSCs with tumor-forming potential in parental 143B cells, thus resulting in reduced tumorsphere formation (Fig. 4D-E). We also observed that 143B-NICD cells were more much resistant than parental cells to the anti-CSCs effect of EC-8042. Finally, in this case we found that the MTM analog was more effective in eliminating CSCs when HES1 was silenced (Fig. 4D-E).

In sum, this gain and loss of function experiments strongly suggest that the inhibition of NOTCH1 pathway plays a key role in the abrogation of stemness activity by EC-8042. Thus, overexpression of NICD

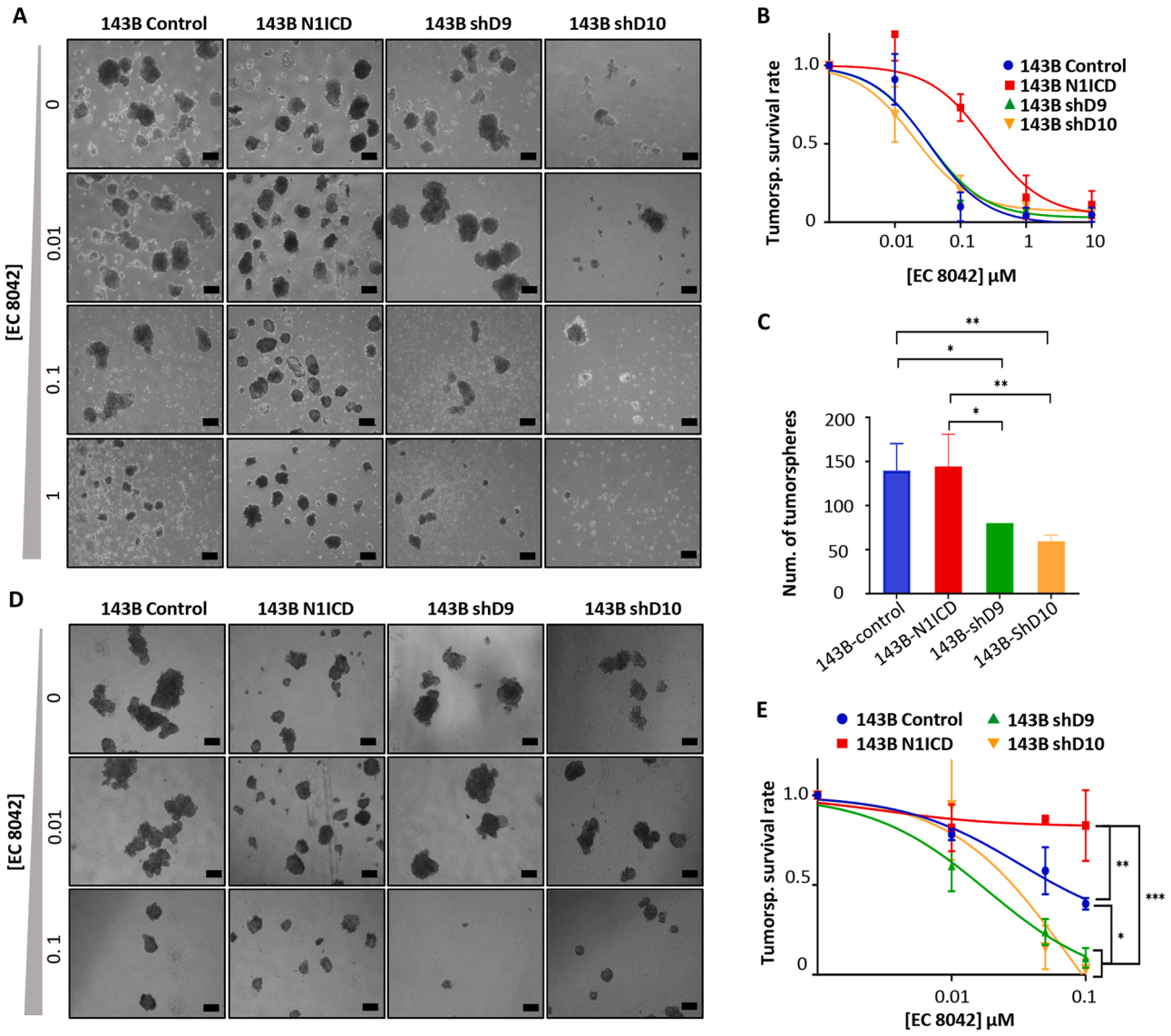

Fig. 4. Effect of EC-842 on osteosarcoma CSCs subpopulations. (A-C) CSC-enriched tumourspheres of parental and NOTCH1-signaling modified 143B cells were treated with increased concentrations of EC-8042 for 72 h. Representative images of the spheres cultures (A), the quantification of the cell viability (WST-1 assay) of spheres (represented as % of control) at the end of the treatment (B) and the counting of number of spheres formed in untreated conditions (C) are shown. (D-E) parental and NOTCH1-signaling modified 143B cells treated with the indicated concentrations of EC-8042 for 48 h were grown in tumorsphere culture conditions for 10 days. Representative images (D) and quantification of cell viability (represented as % of control) of the spheres (E) at the end of the experiment are shown. Scale bars = 250 µm. Error bars represents standard deviation measured from at least three independent replicates and asterisk indicate a statistically significant difference with the control group (*:$p < 0.05$, **:$p < 0.01$; ***:$p < 0.001$ one-way ANOVA).

hamper its anti-tumor action on CSCs, while the silencing of HES1 may cooperate with EC-8042 and render sarcoma CSCs more sensitive to this drug.

3.4. Modulation of NOTCH1 signalling in osteosarcoma cells influences the response to EC-8042 in vivo

Next, we aimed to study whether the modulation of NOTCH signalling also affected tumor growth and the response to EC-8042 in vivo. First, we monitored tumor growth in immunodeficient mice inoculated with parental 143B, 143-NICD, 143B-shD9 or 143B-shD10 cells (Fig. 5A). We found that both cell lines with silenced expression of HES1 grew tumors at a slower rate comparing to parental or NICD-overexpressing cells (Fig. 5A-B). Then, we treated immunodeficient mice carrying xenografts generated by parental 143B, 143B-NICD or 143B-shD10 cells with saline or 18 mg/Kg EC-8042 twice a week. First, the analysis of active NOTCH1 levels in tumors extracted from cohorts of control and treated mice, confirmed that this drug was able to inhibit the expression of NOTCH1 in vivo in parental 143B cells and 143-shD10 cells, but not in 143 cells with forced overexpression of NOTCH1 (Fig. 5C-D and Fig. S6). Then, the analysis of tumor growth evidenced that those tumors generated by 143B-NICD cells showed a poorer response to EC-8042 than those initiated by parental cells. After six doses of treatment with EC-8042, we observed a significant growth reduction in parental tumors (%TGI= 73.8) compared to NICD-overexpressing tumors (%TGI= 56.9%) (Fig. 5E-F). The anti-tumor effect of EC-8042 in tumors generated by HES1-silenced cells (%TGI= 70.0%) was similar to that observed in parental cells. However, the cumulative effect of HES1 depletion and EC-8042 treatment resulted in a lower overall tumor growth rate in 143B-shD10 cells (Fig. 5E-F).

Altogether these data show that the overexpression of NICD reduced anti-tumor activity of EC-8042, most likely by hampering its ability to target CSCs. On the other hand, silencing of HES1 could cooperate with EC-8042 and render sarcoma CSCs more sensitive to this drug.

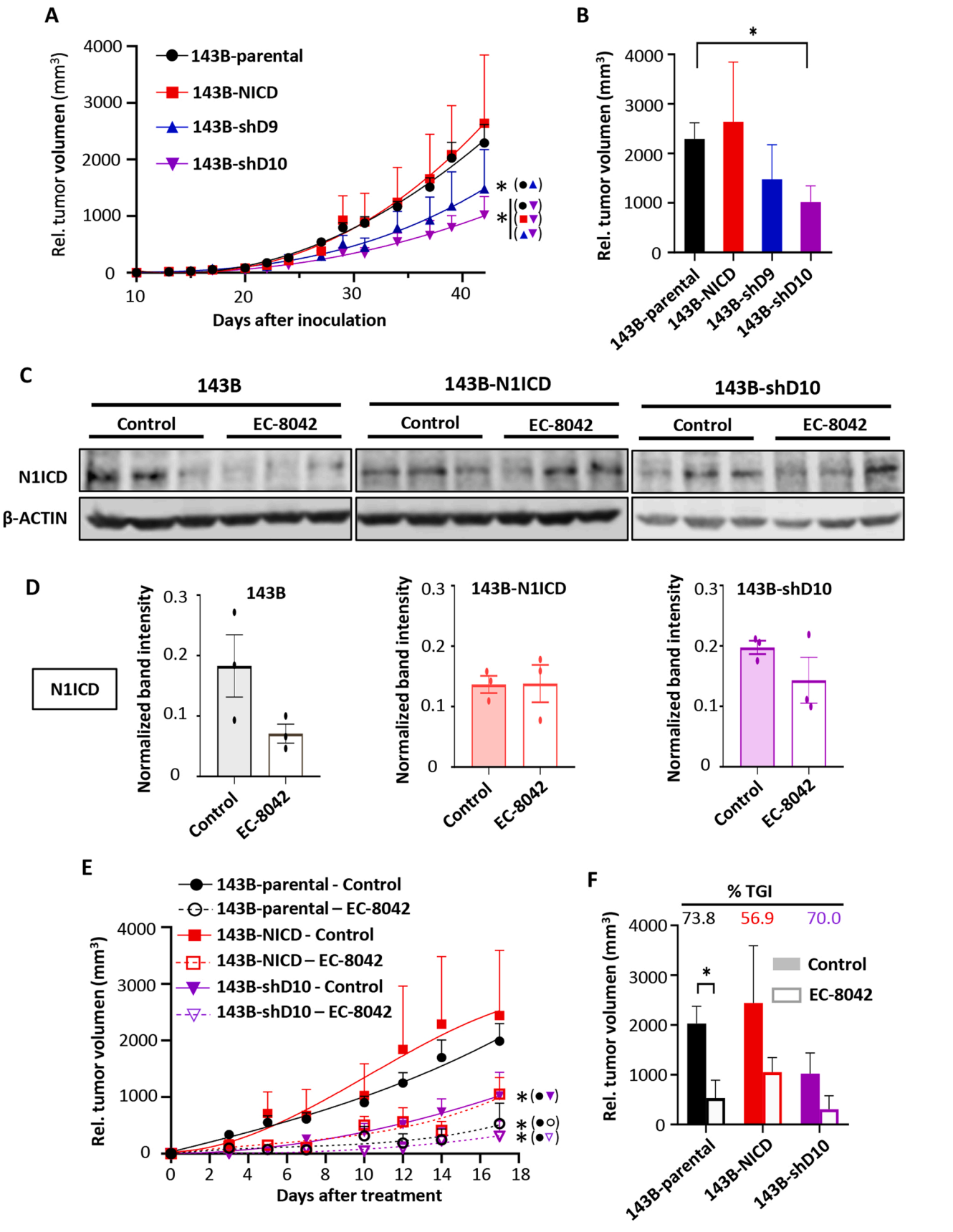

(caption on next page)

Fig. 5. Modulation of NOTCH1 signaling in osteosarcoma cells influences tumor growth and the response to EC-8042 in vivo. A) Curves representing the mean volume of xenograft tumors generated by 143B-parental, 143B-NICD, 143B-shD9 and 143B-shD10 cells (n = 5 per group). B) Mean tumor volumes at the end of the experiment (day 42 after the inoculation). (C-D) Cohorts of mice (n = 3 per group) carrying xenografts generated with 143B-parental, 143B-NICD and 143B-shD10 cells were randomly assigned to receive four doses of saline (control) or 18 mg/Kg EC-8042. Tumors were extracted and processed for protein extraction 24 h after the last dose and the levels of NOTCH1 (N1ICD) were determined by Western blotting (C). The expression of β-actin was used as loading control. Western blotting bands were quantified using Image Studio software and the data were plotted as the means and standard deviations of the ratios of the N1ICD / β-actin band intensities (D). E-F) Xenografts generated with 143B-parental, 143B-NICD and 143B-shD10 cells were randomly assigned to control groups (treated with saline) or groups treated with EC-8042 at 18 mg/Kg twice a week (6 doses) (n = 5 per group). (E) Curves representing the mean relative tumor volume of xenografts during the treatments. (F) Relative tumor volumes at the experimental end point (day 17 after the start of the treatment). Drug efficacy expressed as the percentage of TGI is indicated. Error bars represent the SEM and asterisks indicate statistically significant differences between groups in RM-one way ANOVA (A and E, symbols in brackets indicate the series that are being compared) or in two-sided Student t-tests (B and F) (*:$p < 0.05$).

3.5. NOTCH expression is related with poor prognosis in clinic

Finally, we aimed to investigate whether the levels of active NOTCH1 in sarcoma patients is clinically relevant. Thus, the nuclear expression of this receptor was analyzed by immunohistochemistry in a collection of tissue microarrays, including 82 samples from 10 types of

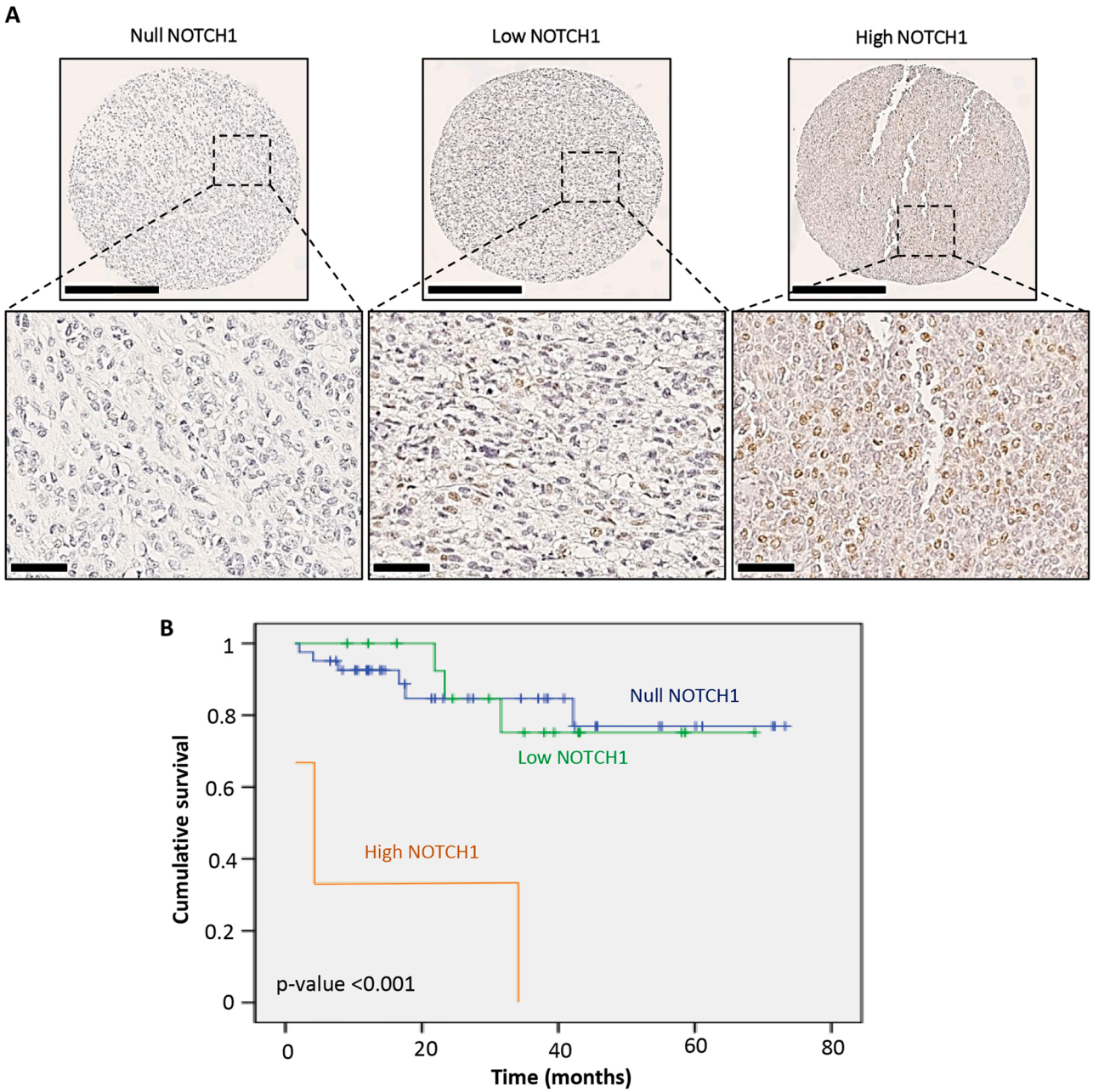

Fig. 6. Immunohistochemical analysis of NOTCH-1 nuclear expression in sarcoma patients and associations with clinical data. (A) Representative examples of the indicated types of sarcomas showing negative, low and high nuclear NOTCH1 staining. Scale bars: 500 (top panels) or 50 μm (bottom panels). (B) Kaplan-Meier cumulative survival curves categorized by NOTCH-1 protein expression in the cohort of sarcoma patients. p-value were estimated using the log-rank test.

sarcomas. Patient specimens were categorized as samples with null, low or high NOTCH1 nuclear expression according to percentage of stained cells and the staining intensity (Fig. 6 A). Low and high NOTCH1 nuclear expression was detected in 19 (23.2%) and 8 (9.8%) sarcoma samples respectively (Table 1). Importantly, NOTCH1 expression correlated with higher tumor grade ($p = 0.001$), poor differentiation ($p = 0.003$) and vascular invasion ($p = 0.037$) (Table 1).

Moreover, those cases with null and low NOTCH1 protein levels showed a longer survival time when compared to those showing a high levels of this factor (61 months (CI 52–70) for null cases; 58 months (CI 48–69) for low expression cases; and 13 months (CI 0–34) for high expression cases) (Fig. 6B). The Hazard Ratio for cases with high levels compared to null cases was 11.095 (CI 2.7–45–6; $p < 0.001$).

In summary, we found that nuclear expression of NOTCH1 correlates with more aggressive tumor phenotypes and a poorer prognosis in sarcoma patients.

4. Discussion

The recent discovery of a close relationship between the usually aggressive evolution of osteosarcomas and the presence of tumor cell subpopulations with CSC phenotypes stresses the need for therapies able to neutralize these CSCs [5,43,44]. In this regard, the MTM analog EC-8042 has emerged as a potent antitumor agent with anti-CSCs activity [29–33,45]. In sarcomas, we have previously shown that EC-8042 demonstrated greater potential to inhibit the tumor growth of soft tissue sarcomas models than doxorubicin. Notably, this antitumor activity was linked to its ability to inhibit the expression and activity of genes associated to the CSC phenotype and with its strong potential to eliminate CSCs in vitro and in vivo [30,31]. In this work, we expand the panel of tumor types in which EC8042 shows anti-CSC activity to include osteosarcomas.

EC-8042 induced a robust pattern of transcriptional repression both in osteosarcoma and liposarcoma cells. Previous studies have reported the ability of EC-8042 to inhibit specific pro-tumor targets in different tumor types. Thus, EC-8042 was able to repress the expression of SRC and PTK2 in head and neck cancer cells [32], VEGFA, TERT and SRC in ovarian cancer [46], WNT5, THBS1, CXCL8, MMP1 and SCG2 in melanoma [27], as well as inhibit SP1-mediated signaling in different tumor types [28,31,46,47]. Our transcriptome analyses also showed that EC-8042 induced an efficient repression of these factors in both liposarcoma and osteosarcoma cells. Among the pathways most robustly repressed by EC-8042, NOTCH1 signaling is known to play oncogenic and pro-stemness roles in many types of tumors [7,13,48]. In osteosarcomas, an aberrant activation of NOTCH signaling could play a role as tumor driver event [8]. In addition, it has been reported that primary osteosarcomas showed increased levels of NOTCH receptors, ligands and downstream target genes, which seems to play a role in the acquisition of drug-resistant phenotypes and in the progression and dissemination of the disease [5,9–11]. Importantly, the survival rate of those patients with high serum levels of NOTCH1 and HES1 was significantly lower than that of the group presenting low levels [49]. In line with these results, our own analysis of NOTCH1 levels in sarcomas samples confirmed that the nuclear protein levels of this receptor correlated with more aggressive phenotypes and poorer disease outcome.

The ability of EC-8042 to inhibit NOTCH1 signaling is also relevant in view of the limitations of the drugs used so far to inhibit this pathway in cancer. Main strategies to inhibit this signaling involve the use of γ-secretase inhibitors or antibodies against NOTCH receptors [7,50]. Although these approaches have been considered for clinical use against different neoplasms, serious side effects observed during clinical trials evidence the narrow therapeutic window for these drugs [50,51]. Therefore, EC-8042 could represent a safer alternative to currently available NOTCH signaling inhibitors. Opposite to other inhibitory strategies, EC-8042 is able to inhibit NOTCH1 signaling at different levels including the NOTCH1 receptor, most of the components of the transcriptional complex of NOTCH and many of the transcriptional targets of the pathways.

Notch signaling have also been involved in mediating stemness phenotypes in osteosarcoma [5,13,52]. Therefore, we explored the hypothesis that the anti-CSC activity of EC-8042 could be mediated by its ability to inhibit NOTCH signaling. Through gain and/or loss of function experiments of NOTCH1 and HES1 in osteosarcoma models we demonstrated that the anti-CSC activity of EC-8042 and the in vivo

Table 1
Distribution of sarcoma cases (N = 82) according to their nuclear levels of NOTCH1 across categories of the indicated patient characteristics and tumor clinicopathologic parameters. P values are shown.

	null NOTCH1 (%)	low NOTCH1 (%)	high NOTCH1 (%)	Total (%)	p (Chi-square)
Cases	55 (67.1)	19 (23.2)	8 (9.8)	82	
Tumor type					
Osteosarcoma	4 (7.3)	3 (15.8)	0 (0)	7 (8.5)	0.014
Ewing Sarcoma	4 (7.3)	1 (5.3)	2 (25.0)	7 (8.5)	
Myxoid Liposarcoma	8 (14.5)	2 (10.5)	0 (0)	10 (12.2)	
Liposarcoma (other subtypes)	8 (14.5)	0 (0)	0 (0)	8 (9.8)	
Chondrosarcoma	9 (16.4)	1 (5.3)	1 (12.5)	11 (13.4)	
Sinovial Sarcoma	3 (5.5)	5 (26.3)	1 (12.5)	9 (11.0)	
Pleomorphic Sarcoma	3 (5.5)	3 (15.8)	4 (50.0)	10 (12.2)	
GIST	3 (5.5)	2 (10.5)	0 (0)	5 (6.1)	
Encondroma	6 (10.9)	0 (0)	0 (0)	6 (7.3)	
Dermatofibrosarcoma	7 (12.7)	2 (10.5)	0	9 (11.0)	
Total	55	19	8	82	
Tumor grade					
1	12 (37.5)	1 (8.3)	0 (0)	13 (25.5)	0.001
2	11 (34.4)	8 (66.7)	0 (0)	19 (37.2)	
3	9 (28.1)	3 (25.0)	7 (100)	19 (37.2)	
Total	32	12	7	51	
Differentiation					
Well differentiated	10 (40.0)	0 (0)	0 (0)	10 (23.8)	0.003
Moderately different.	0 (0)	3 (27.3)	0 (0)	3 (7.1)	
Poorly differentiated	15 (60.0)	8 (72.7)	6 (100)	29 (69.0)	
Total	25	11	6	42	
Vascular invasion					
No	30 (93.75)	10 (83.3)	4 (57.1)	44 (86.3)	0.037
Yes	2 (6.25)	2 (16.7)	3 (42.9)	7 (13.7)	
Total	32	12	7	51	

response to this drug highly rely on its ability to repress this pathway. In line with this results, previous studies using γ-secretase inhibitors to treat osteosarcoma cells also showed that inhibition of NOTCH signaling resulted in reduced CSC activity and the reversion of resistant phenotypes [12,13,53].

Altogether, these results suggest that EC-8042 could represent a suitable therapeutic option to eliminate CSCs in osteosarcomas and other tumor types where NOTCH signaling may play a pro-tumorigenic role.

Ethics approval and consent to participate

All experimental protocols have been performed in accordance with institutional review board guidelines and were approved by the Institutional Ethics Committee of the Principado de Asturias (ref. 255/19) and the Animal Research Ethical Committee of the University of Oviedo (ref. PROAE 34–2019).

Funding

This work was supported by the Agencia Estatal de Investigación (AEI) [MICINN/Fondo Europeo de Desarrollo Regional (FEDER) (grant PID2019–106666RB-I00 to R.R.) and ISC III/FEDER (Consorcio CIBERONC - CB16/12/00390)] and the Plan de Ciencia Tecnología e Innovación del Principado de Asturias/FEDER [grant IDI/2021/000027 and Severo Ochoa predoctoral fellowships BP-17–108 to O.E., BP-20–046 to B.G. and BP-21–084 to DM].

CRediT authorship contribution statement

OE: development of methodology, performance of experimental procedures, acquisition, analysis and interpretation of data and manuscript draft writing. VR, JT and VA: development of methodology, performance of experimental procedures, acquisition, analysis and interpretation of data. DZ, BG, CH, AR and JG-M: performance of experimental procedures. FM, AB and VR-M: provision of key materials, analysis and interpretation of data and manuscript revision. VBL and MVG: analysis and interpretation of data and manuscript revision. RR: conception and design, analysis and interpretation of data, manuscript writing, supervision and financial support. All authors have read and approved the manuscript.

Acknowledements

We are grateful to Mar Rodríguez-Santamaría (Animal Research facilities, ISPA) for her assistance with the in vivo experiments.

Conflict of interest statement

The authors declare the following financial interests/personal relationships which may be considered as potential competing interests: Francisco Moris was an employee and reported ownership of stock in of EntreChem SL until April 2022. All other authors declare they have no competing interests.

Data availability

The RNA seq datasets supporting the conclusions of this article are available in the GEO-NCBI repository (Reference: GSE161616; https://www.ncbi.nlm.nih.gov/geo/query/acc.cgi?acc=GSE161616).

Appendix A. Supporting information

Supplementary data associated with this article can be found in the online version at doi:10.1016/j.biopha.2023.114627.

References

[1] T.G. Grunewald, M. Alonso, S. Avnet, A. Banito, S. Burdach, F. Cidre-Aranaz, G. Di Pompo, M. Distel, H. Dorado-Garcia, J. Garcia-Castro, L. Gonzalez-Gonzalez, A. E. Grigoriadis, M. Kasan, C. Koelsche, M. Krumbholz, F. Lecanda, S. Lemma, D. L. Longo, C. Madrigal-Esquivel, A. Morales-Molina, J. Musa, S. Ohmura, B. Ory, M. Pereira-Silva, F. Perut, R. Rodriguez, C. Seeling, N. Al Shaaili, S. Shaabani, K. Shiavone, S. Sinha, E.M. Tomazou, M. Trautmann, M. Vela, Y.M. Versleijen-Jonkers, J. Visgauss, M. Zalacain, S.J. Schober, A. Lissat, W.R. English, N. Baldini, D. Heymann, Sarcoma treatment in the era of molecular medicine, EMBO Mol. Med. 12 (11) (2020), e11131.

[2] L.R. Sadykova, A.I. Ntekim, M. Muyangwa-Semenova, C.S. Rutland, J. N. Jeyapalan, N. Blatt, A.A. Rizvanov, Epidemiology and risk factors of osteosarcoma, Cancer Investig. 38 (5) (2020) 259–269.

[3] P.G. Casali, S. Bielack, N. Abecassis, H.T. Aro, S. Bauer, R. Biagini, S. Bonvalot, I. Boukovinas, J. Bovee, B. Brennan, T. Brodowicz, J.M. Broto, L. Brugieres, A. Buonadonna, E. De Alava, A.P. Dei Tos, X.G. Del Muro, P. Dileo, C. Dhooge, M. Eriksson, F. Fagioli, A. Fedenko, V. Ferraresi, A. Ferrari, S. Ferrari, A.M. Frezza, N. Gaspar, S. Gasperoni, H. Gelderblom, T. Gil, G. Grignani, A. Gronchi, R.L. Haas, B. Hassan, S. Hecker-Nolting, P. Hohenberger, R. Issels, H. Joensuu, R.L. Jones, I. Judson, P. Jutte, S. Kaal, L. Kager, B. Kasper, K. Kopeckova, D.A. Krakorova, R. Ladenstein, A. Le Cesne, I. Lugowska, O. Merimsky, M. Montemurro, B. Morland, M.A. Pantaleo, R. Piana, P. Picci, S. Piperno-Neumann, A.L. Pousa, P. Reichardt, M. H. Robinson, P. Rutkowski, A.A. Safwat, P. Schoffski, S. Sleijfer, S. Stacchiotti, S. J. Strauss, K. Sundby Hall, M. Unk, F. Van Coevorden, W.T.A. van der Graaf, J. Whelan, E. Wardelmann, O. Zaikova, J.Y. Blay, P. Esmo, E. Ern, Guidelines Committee, Bone sarcomas: ESMO-PaedCan-EURACAN clinical practice guidelines for diagnosis, treatment and follow-up, Ann. Oncol. 29 (Suppl 4) (2018) iv79–iv95.

[4] A. Abarrategi, J. Tornin, L. Martinez-Cruzado, A. Hamilton, E. Martinez-Campos, J. P. Rodrigo, M.V. González, N. Baldini, J. Garcia-Castro, R. Rodriguez, Osteosarcoma: cells-of-origin, cancer stem cells, and targeted therapies, Stem Cells Int. 2016 (2016) 3631764.

[5] S.T. Menéndez, B. Gallego, D. Murillo, A. Rodríguez, R. Rodríguez, Cancer stem cells as a source of drug resistance in bone sarcomas, J. Clin. Med. 10 (12) (2021).

[6] R. Rodríguez, J. Hatina, S. Gambera, S.T. Menéndez, J. García-Castro, Chapter 28 - Cancer stem cells and clonal evolution in bone sarcomas, in: D. Heymann (Ed.), *Bone Sarcomas and Bone Metastases - From Bench to Bedside, Third edition.*,, Academic Press, 2022, pp. 371–391.

[7] X. Yuan, H. Wu, H. Xu, H. Xiong, Q. Chu, S. Yu, G.S. Wu, K. Wu, Notch signaling: an emerging therapeutic target for cancer treatment, Cancer Lett. 369 (1) (2015) 20–27.

[8] J. Tao, M.M. Jiang, L. Jiang, J.S. Salvo, H.C. Zeng, B. Dawson, T.K. Bertin, P. H. Rao, R. Chen, L.A. Donehower, F. Gannon, B.H. Lee, Notch activation as a driver of osteogenic sarcoma, Cancer Cell 26 (3) (2014) 390–401.

[9] Y. Gao, L. Bai, G. Shang, Notch-1 promotes the malignant progression of osteosarcoma through the activation of cell division cycle 20, Aging (Albany NY) 13 (2) (2020) 2668–2680.

[10] M.M. McManus, K.R. Weiss, D.P. Hughes, Understanding the role of Notch in osteosarcoma, Adv. Exp. Med. Biol. 804 (2014) 67–92.

[11] L. Yu, K. Xia, T. Gao, J. Chen, Z. Zhang, X. Sun, B.M. Simões, R. Eyre, Z. Fan, W. Guo, R.B. Clarke, The Notch Pathway Promotes Osteosarcoma Progression through Activation of Ephrin Reverse Signaling, Mol. Cancer Res 17 (12) (2019) 2383–2394.

[12] J. Yang, W. Guo, L. Wang, L. Yu, H. Mei, S. Fang, A. Chen, Y. Liu, K. Xia, G. Liu, Notch signaling is important for epithelial-mesenchymal transition induced by low concentrations of doxorubicin in osteosarcoma cell lines, Oncol. Lett. 13 (4) (2017) 2260–2268.

[13] L. Yu, Z. Fan, S. Fang, J. Yang, T. Gao, B.M. Simões, R. Eyre, W. Guo, R.B. Clarke, Cisplatin selects for stem-like cells in osteosarcoma by activating Notch signaling, Oncotarget 7 (22) (2016) 33055–33068.

[14] C. Vizcaíno, S. Mansilla, J. Portugal, Sp1 transcription factor: a long-standing target in cancer chemotherapy, Pharm. Ther. 152 (2015) 111–124.

[15] D.M. Miller, D.A. Polansky, S.D. Thomas, R. Ray, V.W. Campbell, J. Sanchez, C. A. Koller, Mithramycin selectively inhibits transcription of G-C containing DNA, Am. J. Med Sci. 294 (5) (1987) 388–394.

[16] P. Dong, Y. Xiong, S.J.B. Hanley, J. Yue, H. Watari, Musashi-2, a novel oncoprotein promoting cervical cancer cell growth and invasion, is negatively regulated by p53-induced miR-143 and miR-107 activation, J. Exp. Clin. Cancer Res. 36 (1) (2017) 150.

[17] Ó. Estupiñán, E. Niza, I. Bravo, V. Rey, J. Tornín, B. Gallego, P. Clemente-Casares, F. Moris, A. Ocaña, V. Blanco-Lorenzo, M. Rodríguez-Santamaría, A. Vallina-Álvarez, M.V. González, A. Rodríguez, D. Hermida-Merino, C. Alonso-Moreno, R. Rodríguez, Mithramycin delivery systems to develop effective therapies in sarcomas, J. Nanobiotechnol. 19 (1) (2021) 267.

[18] Ó. Estupiñán, C. Rendueles, P. Suárez, V. Rey, D. Murillo, F. Morís, G. Gutiérrez, M. M.d.C. Blanco-López, R.Rodríguez Matos, Nano-Encapsulation Mithramycin Transf. Polym. Micelles Treat. Sarcomas 10 (7) (2021) 1358.

[19] W. Quarni, R. Dutta, R. Green, S. Katiri, B. Patel, S.S. Mohapatra, S. Mohapatra, Mithramycin a inhibits colorectal cancer growth by targeting cancer stem cells, Sci. Rep. 9 (1) (2019) 15202.

[20] S. Saha, S. Mukherjee, M. Mazumdar, A. Manna, P. Khan, A. Adhikary, K. Kajal, D. Jana, G. Sa, S. Mukherjee, D.K. Sarkar, T. Das, Mithramycin A sensitizes therapy-resistant breast cancer stem cells toward genotoxic drug doxorubicin, Transl. Res. 165 (5) (2015) 558–577.

[21] D.K. Singh, R.K. Kollipara, V. Vemireddy, X.L. Yang, Y. Sun, N. Regmi, S. Klingler, K.J. Hatanpaa, J. Raisanen, S.K. Cho, S. Sirasanagandla, S. Nannepaga, S. Piccirillo,

T. Mashimo, S. Wang, C.G. Humphries, B. Mickey, E.A. Maher, H. Zheng, R.S. Kim, R. Kittler, R.M. Bachoo, Oncogenes activate an autonomous transcriptional regulatory circuit that drives glioblastoma, Cell Rep. 18 (4) (2017) 961–976.
[22] R.J. Vanner, M. Remke, M. Gallo, H.J. Selvadurai, F. Coutinho, L. Lee, M. Kushida, R. Head, S. Morrissy, X. Zhu, T. Aviv, V. Voisin, I.D. Clarke, Y. Li, A.J. Mungall, R. A. Moore, Y. Ma, S.J. Jones, M.A. Marra, D. Malkin, P.A. Northcott, M. Kool, S. M. Pfister, G. Bader, K. Hochedlinger, A. Korshunov, M.D. Taylor, P.B. Dirks, Quiescent sox2(+) cells drive hierarchical growth and relapse in sonic hedgehog subgroup medulloblastoma, Cancer Cell 26 (1) (2014) 33–47.
[23] C. Méndez, J. González-Sabín, F. Morís, J.A. Salas, Expanding the chemical diversity of the antitumoral compound mithramycin by combinatorial biosynthesis and biocatalysis: the quest for mithralogs with improved therapeutic window, Planta Med. 81 (15) (2015) 1326–1338.
[24] L.E. Núñez, S.E. Nybo, J. González-Sabín, M. Pérez, N. Menéndez, A.F. Braña, K. A. Shaaban, M. He, F. Morís, J.A. Salas, J. Rohr, C. Méndez, A novel mithramycin analogue with high antitumor activity and less toxicity generated by combinatorial biosynthesis, J. Med. Chem. 55 (12) (2012) 5813–5825.
[25] L.E. Núñez, S.E. Nybo, J. González-Sabín, M. Pérez, N. Menéndez, A.F. Braña, K. A. Shaaban, M. He, F. Morís, J.A. Salas, J. Rohr, C. Méndez, A novel mithramycin analogue with high antitumor activity and less toxicity generated by combinatorial biosynthesis, J. Med. Chem. 55 (12) (2012) 5813–5825.
[26] C.L. Osgood, N. Maloney, C.G. Kidd, S. Kitchen-Goosen, L. Segars, M. Gebregiorgis, G.M. Woldemichael, M. He, S. Sankar, S.L. Lessnick, M. Kang, M. Smith, L. Turner, Z.B. Madaj, M.E. Winn, L.-E. Núñez, J. González-Sabín, L.J. Helman, F. Morís, P. J. Grohar, Identification of mithramycin analogues with improved targeting of the EWS-FLI1 transcription factor. clinical cancer research: an official journal of the American Association for, Cancer Res. 22 (16) (2016) 4105–4118.
[27] A. Federico, T. Steinfass, L. Larribère, D. Novak, F. Morís, L.-E. Núñez, V. Umansky, J. Utikal, Mithramycin A and Mithralog EC-8042 Inhibit SETDB1 Expression and Its Oncogenic Activity in Malignant Melanoma, Mol. Ther. - Oncolytics 18 (2020) 83–99.
[28] C. Vizcaíno, L.E. Núñez, F. Morís, J. Portugal, Genome-wide modulation of gene transcription in ovarian carcinoma cells by a new mithramycin analogue, PLoS One 9 (8) (2014), e104687.
[29] A. Pandiella, F. Morís, A. Ocaña, L.-E. Núñez, J.C. Montero, Antitumoral activity of the mithralog EC-8042 in triple negative breast cancer linked to cell cycle arrest in G2, Oncotarget 6 (32) (2015) 32856–32867.
[30] S.T. Menendez, V. Rey, L. Martinez-Cruzado, M.V. Gonzalez, A. Morales-Molina, L. Santos, V. Blanco, C. Alvarez, O. Estupiñan, E. Allonca, J.P. Rodrigo, J. García-Castro, J.M. Garcia-Pedrero, R. Rodriguez, SOX2 Expression and Transcriptional Activity Identifies a Subpopulation of Cancer Stem Cells in Sarcoma with Prognostic Implications, Cancers (Basel) 12 (4) (2020).
[31] J. Tornin, L. Martinez-Cruzado, L. Santos, A. Rodriguez, L.E. Nunez, P. Oro, M. A. Hermosilla, E. Allonca, M.T. Fernandez-Garcia, A. Astudillo, C. Suarez, F. Moris, R. Rodriguez, Inhibition of SP1 by the mithramycin analog EC-8042 efficiently targets tumor initiating cells in sarcoma, Oncotarget 7 (21) (2016) 30935–30950.
[32] F. Hermida-Prado, M.Á. Villaronga, R. Granda-Díaz, N. del-Río-Ibisate, L. Santos, M.A. Hermosilla, P. Oro, E. Allonca, J. Agorreta, I. Garmendia, J. Tornín, J. Perez-Escuredo, R. Fuente, L.M. Montuenga, F. Morís, J.P. Rodrigo, R. Rodríguez, J. M. García-Pedrero, The SRC inhibitor dasatinib induces stem cell-like properties in head and neck cancer cells that are effectively counteracted by the mithralog EC-8042, 8 (8) (2019) 1157.
[33] D. Shinde, D. Albino, M. Zoma, A. Mutti, S.N. Mapelli, G. Civenni, A. Kokanovic, J. Merulla, J. Perez-Escuredo, P. Costales, F. Morìs, C.V. Catapano, G.M. Carbone, Transcriptional reprogramming and inhibition of tumor-propagating stem-like cells by EC-8042 in ERG-positive Prostate Cancer. European Urology, Oncology 2 (4) (2019) 415–424.
[34] A. Alfranca, L. Martinez-Cruzado, J. Tornin, A. Abarrategi, T. Amaral, E. de Alava, P. Menendez, J. Garcia-Castro, R. Rodriguez, Bone microenvironment signals in osteosarcoma development, Cell Mol. Life Sci. 72 (16) (2015) 3097–3113.
[35] R. Rodriguez, M. Rosu-Myles, M. Aráuzo-Bravo, A. Horrillo, Q. Pan, E. Gonzalez-Rey, M. Delgado, P. Menendez, Human bone marrow stromal cells lose immunosuppressive and anti-inflammatory properties upon oncogenic transformation, Stem Cell Rep. 3 (4) (2014) 606–619.
[36] R. Rodriguez, J. Tornin, C. Suarez, A. Astudillo, R. Rubio, C. Yauk, A. Williams, M. Rosu-Myles, J.M. Funes, C. Boshoff, P. Menendez, Expr. FUS-CHOP Fusion Protein Immortal. /Transform. Hum. mesenchymal stem Cells Drives mixoid liposarcoma Form. 31 (10) (2013) 2061–2072.
[37] O. Estupiñan, L. Santos, A. Rodriguez, L. Fernandez-Nevado, P. Costales, J. Perez-Escuredo, M.A. Hermosilla, P. Oro, V. Rey, J. Tornin, E. Allonca, M.T. Fernandez-Garcia, C. Alvarez-Fernandez, A. Braña, A. Astudillo, S.T. Menendez, F. Moris, R. Rodriguez, The multikinase inhibitor EC-70124 synergistically increased the antitumor activity of doxorubicin in sarcomas, Int. J. Cancer 145 (1) (2019) 254–266.
[38] L. Martinez-Cruzado, J. Tornin, A. Rodriguez, L. Santos, E. Allonca, M. T. Fernandez-Garcia, A. Astudillo, J.M. Garcia-Pedrero, R. Rodriguez, Trabectedin and campthotecin synergistically eliminate cancer stem cells in cell-of-origin sarcoma models, Neoplasia 19 (6) (2017) 460–470.
[39] B. Gallego, D. Murillo, V. Rey, C. Huergo, O. Estupinan, A. Rodriguez, J. Tornin, R. Rodriguez, Addressing doxorubicin resistance in bone sarcomas using novel drug-resistant models, Int. J. Mol. Sci. 23 (12) (2022).
[40] P. Zuazua-Villar, R. Rodriguez, M.E. Gagou, P.A. Eyers, M. Meuth, DNA replication stress in CHK1-depleted tumour cells triggers premature (S-phase) mitosis through inappropriate activation of Aurora kinase B, Cell Death Dis. 5 (2014), e1253.
[41] J. Tornin, F. Hermida-Prado, R.S. Padda, M.V. Gonzalez, C. Alvarez-Fernandez, V. Rey, L. Martinez-Cruzado, O. Estupiñan, S.T. Menendez, L. Fernandez-Nevado, A. Astudillo, J.P. Rodrigo, F. Lucien, Y. Kim, H.S. Leong, J.M. Garcia-Pedrero, R. Rodriguez, FUS-CHOP promotes invasion in myxoid liposarcoma through a SRC/FAK/RHO/ROCK-dependent pathway, Neoplasia 20 (1) (2018) 44–56.
[42] L. Martinez-Cruzado, J. Tornin, L. Santos, A. Rodriguez, J. García-Castro, F. Morís, R. Rodriguez, Aldh1 expression and activity increase during tumor evolution in sarcoma cancer stem cell populations, Sci. Rep. 6 (1) (2016) 27878.
[43] J. Hatina, M. Kripnerova, K. Houfkova, M. Pesta, J. Kuncova, J. Sana, O. Slaby, R. Rodríguez, in: A. Birbrair (Ed.), *Sarcoma Stem Cell Heterogeneity*, in *Stem Cells Heterogeneity - Novel Concepts*, Springer International Publishing, Cham., 2019, pp. 95–118.
[44] K. Schiavone, D. Garnier, M.-F. Heymann, D. Heymann, The Heterogeneity of Osteosarcoma, in: A. Birbrair (Ed.), *The Role Played by Cancer Stem Cells*, in *Stem Cells Heterogeneity in Cancer*, Springer International Publishing, Cham., 2019, pp. 187–200.
[45] D. Schweer, J.R. McCorkle, J. Rohr, O.V. Tsodikov, F. Ueland, J. Kolesar, Mithramycin and Analogs for Overcoming Cisplatin Resistance in Ovarian Cancer, in: Biomedicines, 9, 2021, p. 70.
[46] A. Fernández-Guizán, A. López-Soto, A. Acebes-Huerta, L. Huergo-Zapico, M. Villa-Álvarez, L.-E. Núñez, F. Morís, S. Gonzalez, Pleiotropic Anti-Angiogenic and Anti-Oncogenic Activities of the Novel Mithralog Demycarosyl-3D-ß-D-Digitoxosyl-Mithramycin SK (EC-8042), PLOS ONE 10 (11) (2015), e0140786.
[47] A. Fernández-Guizán, S. Mansilla, F. Barceló, C. Vizcaíno, L.E. Núñez, F. Morís, S. González, J. Portugal, The activity of a novel mithramycin analog is related to its binding to DNA, cellular accumulation, and inhibition of Sp1-driven gene transcription, Chem. Biol. Inter. 219 (2014) 123–132.
[48] O. Meurette, P. Mehlen, Notch signaling in the tumor microenvironment, Cancer Cell 34 (4) (2018) 536–548.
[49] L. Fang, B. Li, D. Yu, B. Wang, T. Zhao, Analysis of changes in the expression of Notch1 and HES1 and the prognosis of osteosarcoma patients following surgery, Oncol. Lett. 20 (4) (2020) 29.
[50] V. Venkatesh, R. Nataraj, G.S. Thangaraj, M. Karthikeyan, A. Gnanasekaran, S. B. Kaginelli, G. Kuppanna, C.G. Kallappa, K.M. Basalingappa, Targeting Notch signalling pathway of cancer stem cells, Stem Cell Invest. 5 (2018) 5.
[51] N. Takebe, L. Miele, P.J. Harris, W. Jeong, H. Bando, M. Kahn, S.X. Yang, S.P. Ivy, Targeting Notch, Hedgehog, and Wnt pathways in cancer stem cells: clinical update, Nat. Rev. Clin. Oncol. 12 (8) (2015) 445–464.
[52] J. Lu, G. Song, Q. Tang, J. Yin, C. Zou, Z. Zhao, X. Xie, H. Xu, G. Huang, J. Wang, D. F. Lee, R. Khokha, H. Yang, J. Shen, MiR-26a inhibits stem cell-like phenotype and tumor growth of osteosarcoma by targeting Jagged1, Oncogene 36 (2) (2017) 231–241.
[53] G. Dai, S. Deng, W. Guo, L. Yu, J. Yang, S. Zhou, T. Gao, Notch pathway inhibition using DAPT, a γ-secretase inhibitor (GSI), enhances the antitumor effect of cisplatin in resistant osteosarcoma, Mol. Carcinog. 58 (1) (2019) 3–18.